Applied Energy 380 (2025) 125069

Contents lists available at ScienceDirect

Applied Energy

journal homepage: www.elsevier.com/locate/apenergy

Validity ranges of locational marginal emission factors for the environmental assessment of electric load shifting

B. Nilges, A. Haese, C. Reinert, N. von der Assen *

Institute of Technical Thermodynamics, RWTH Aachen University, Schinkelstraße 8, 52062 Aachen, Germany

HIGHLIGHTS

- Grid congestions increase relevance of regionally-resolved environmental assessment.
- Locational marginal emission factors are well suited to reveal regional differences.
- Regionally-resolved environmental assessment in optimal power flow model.
- Validity ranges of locational marginal emission factors are small.
- Battery projects cannot be assessed with locational marginal emission factors.

GRAPHICAL ABSTRACT

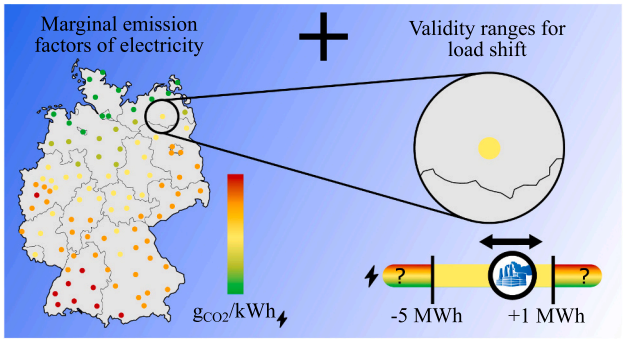

ARTICLE INFO

Keywords:
Demand-side management
Electrical storage
Electric power system
Environmental assessment
Greenhouse gas emissions
Energy system optimization model

ABSTRACT

The integration of volatile renewable energies into electric power systems requires the synchronization of electricity supply and demand through load shifting by demand-side management and electrical storage. Although the environmental impacts of load shifting are widely discussed in the literature, there is only limited research on location-specific differences that are inherent in large-scale electric power systems. For a location-specific environmental assessment, locational marginal emission factors (MEFs) can be determined in power flow models. However, the locational MEFs are derived for an infinitesimal change in load and, thus, are not necessarily applicable for the assessment of large load shifts. In this paper, we provide validity ranges for the locational MEFs to determine for which load changes the MEFs are exact. We analyze the locational MEFs and the validity ranges on a model of the German electric power system. Consistent with literature, the results show that the locational MEFs can vary between −144 g_{CO2}/kWh and 2620 g_{CO2}/kWh in the case of severe grid congestion. However, we show that validity ranges of the locational MEFs are rather small with values of mostly around 5 MW and in some cases even reach zero. Therefore, we conclude that while locational MEFs are important for the location-specific assessment of load shifting, the relatively small validity ranges of locational MEFs must also be considered when large load shifts are evaluated.

* Corresponding author.
E-mail address: niklas.vonderassen@ltt.rwth-aachen.de (N. von der Assen).

https://doi.org/10.1016/j.apenergy.2024.125069
Received 13 September 2024; Received in revised form 4 November 2024; Accepted 30 November 2024
Available online 9 December 2024
0306-2619/© 2024 The Authors. Published by Elsevier Ltd. This is an open access article under the CC BY license (http://creativecommons.org/licenses/by/4.0/).

1. Introduction

In order to reduce the CO_2 emissions of large-scale electric power systems, renewable energies are increasingly integrated into electric power systems [24]. Due to fluctuations in electricity generation from volatile renewable energies, load shifting by flexibly operated processes, such as demand-side management and electrical storage, is necessary to synchronize electricity generation with demand [20,34,45]. While the synchronization of electricity generation and demand is necessary for security of supply, the general goal to reduce CO_2 emissions in the electric power system still holds. Therefore, the environmental assessment of load shifting in future electric power systems is a key research topic [31]. In particular, such environmental assessments need to consider location-specific aspects, as the environmental benefit of load shifting varies with the location [6].

Environmental assessment studies on flexibly operated processes generally utilize time-dependent emission factors of electricity generation to account for time-varying emissions in the electric power system [16,27,28,49]. Time-dependent emission factors of electricity generation can be classified into time-dependent average emission factors (AEF), which quantify the average emissions of the total electricity generation in the system, and time-dependent marginal emission factors (MEF), which quantify the emissions arising due to an infinitesimal change in the system's electricity demand (Fig. 1).

In most environmental assessments of flexibly operated processes, AEFs are applied due to their simple calculation [13,27,28,49,55]. However, AEFs do not represent the actual response of power plants to the flexible operation of processes as market effects in the electric power system are not considered (e.g., power plants are typically dispatched depending on their cost of operation). Therefore, AEFs should primarily be used for emission accounting and not for strategic decision support. For strategic decision support, MEFs are recommended [25], which are also applied for example in consequential life cycle assessment [33].

Various calculation methods have been presented to identify the power plants that respond to a marginal change in demand in order to determine MEFs:

1. Regression models based on historical electricity market data [14,18,47,48,50].
2. Economic dispatch models based on the merit order of the power plants [1,2,12,40].
3. Optimization models using a marginal increase in demand between optimization runs to compute the power plant response [4].

However, these methods are either not applicable for the assessment of load shifting in future electric power systems (1), cannot consider locational-aspects (2) or are computationally too expensive when considering locational-aspects (3).

The locational-aspects can be considered by applying location- and time-dependent MEFs. These locational MEFs represent the emissions that arise from the change in demand at a specific location in the electric power system. Therefore, locational MEFs do not only provide one emission factor for the entire electric power system but provide one emission factor for every considered location in the electric power system. Several studies develop regression-based methods to determine locational MEFs [9,17,38]. However, these methods are based on historical data and are, therefore, not applicable for the analysis of future electric power systems. Ruiz and Rudkevich [43] overcome these issues by providing a method to calculate location- and time-dependent MEFs in an optimal power flow model. The locational MEFs are mathematically derived from the results of a linear optimization problem of a spatially-resolved electric power system and can also be applied on future systems. This conceptual approach is already applied in several studies, e.g., for the assessment of investment policies [42], carbon displacement strategies [19], spatial load shifting by data centers [32], temporal load shifting in distribution networks [36], and as a basis for dynamic locational MEFs [52]. Furthermore, locational MEFs are already utilized in the industry for the environmental assessment of decarbonization measures such as solar projects [35].

Locational MEFs provide a snapshot of the complex system behavior and, thus, the range in which the MEFs are exact is, by definition, not given. However, in electric power systems, the marginal power plant only reacts to a change in demand until a technical constraint is reached (e.g., the power plants capacity limit). When a technical constraint is reached, the marginal power plant changes and the previously determined locational MEFs are no longer exact. However, for the environmental assessment of load shifting, the locational MEFs need to be exact to enable an accurate environmental assessment for decision support. For locational MEFs, the change in demand until a technical constraint is reached can be determined and these ranges of demand change could actually be used to analyze whether the MEFs are suitable for the environmental assessment of large load shifts, as in the case of battery projects with around 20 MW of electric power [30]. However, while the range is unknown, the accuracy of every environmental assessment using locational MEFs can be challenged.

In this work, we determine validity ranges for locational MEFs and analyze their applicability to assess large load shifts. First, we provide the general problem formulation, the calculation method for the locational MEFs, and the method to determine validity ranges for the locational MEFs (Section 2). These validity ranges determine the amount of

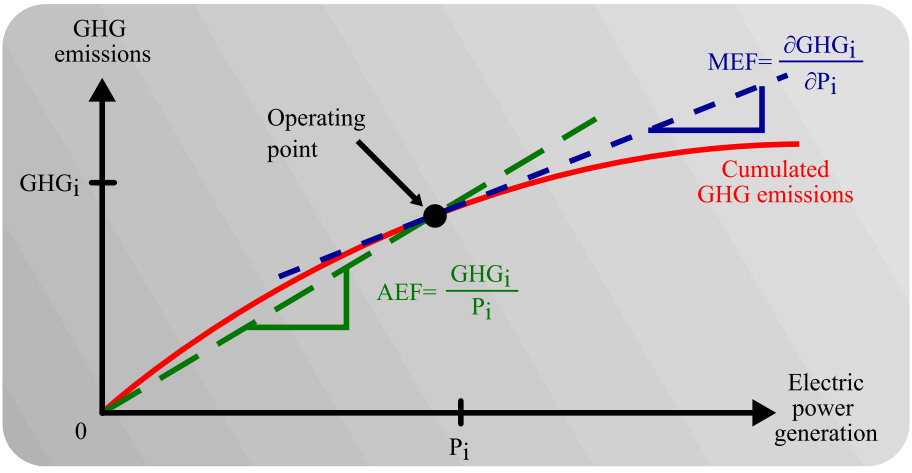

Fig. 1. General concepts of average emission factor (AEF) and marginal emission factor (MEF) described on a cumulated GHG emissions graph of an exemplary electric power system.

demand that can be increased or decreased at a specific location while the MEFs remains constant. We demonstrate the calculation of locational MEFs with validity ranges on a spatially and temporally resolved model of the German electric power system which is described in Section 3. Then, we analyze the locational emission factors for the German electric power system and discuss the resulting validity ranges and their implications for the environmental assessment of load shifting (Section 4). Finally, we conclude our work in Section 5.

2. Method

The calculation of locational MEFs and validity ranges is based on an optimal power flow model. In this section, we first describe the optimal power flow model (Section 2.1), followed by the mathematical derivation of locational MEFs as currently used in the literature (Section 2.2). Then, we introduce the validity ranges for locational MEFs by using the method of ranging (Section 2.3).

2.1. Optimal power flow model

The locational MEFs are determined in a linear optimization model in which power plants are dispatched at different locations in the electric power system and electricity is transmitted via power lines between the locations. A general approach to model power plant dispatch and electricity transmission in large-scale electric power systems is an optimal power flow model. The optimal power flow model is a non-linear optimization problem that uses a grid structure of nodes, where electricity is generated or demanded, and power lines, which are used for electricity transmission between two nodes. For high voltage electricity transmission, the power flow model can be linearized to the direct current load flow model as the following assumptions hold true [39]:

1. Voltage angles are small
2. Line resistance is negligible
3. Voltage profile is flat

The linear direct current load flow model can be formulated in vector notation as follows (bold letters for vectors and matrices, non-vector formulation in Supplementary Information).

$$\min \quad \boldsymbol{C} = \boldsymbol{c}^{\mathrm{T}}\boldsymbol{P} \tag{1}$$

$$\text{s.t.} \quad \boldsymbol{P} + \boldsymbol{\Psi\theta} = \boldsymbol{D} \tag{1a}$$

$$\boldsymbol{0} \leq \boldsymbol{P} \leq \boldsymbol{\Gamma} \tag{1b}$$

$$-\boldsymbol{\Omega} \leq \boldsymbol{\Phi\theta} \leq \boldsymbol{\Omega} \tag{1c}$$

$$\theta_{\mathrm{ref}} = 0 \tag{1d}$$

The objective is to minimize the overall cost of electricity generation $\boldsymbol{C}$ that is determined by multiplying the generator-specific costs $\boldsymbol{c}^{\mathrm{T}}$ by the electricity generation $\boldsymbol{P}$ (Eq. 1). The objective function is subject to various constraints (Eqs. 1a-1d). In the energy balance (Eq. 1a), the electricity generation at a specific node and electricity transmission from or to the node must meet the electricity demand $\boldsymbol{D}$. The electricity transmission from or to a node is determined by the product of the node-specific susceptance matrix $\boldsymbol{\Psi}$ times the phase angles $\boldsymbol{\theta}$. Furthermore, electricity generation is limited by the electricity generation capacities $\boldsymbol{\Gamma}$ (Eq. 1b). Likewise, the electricity transmission over the power lines, expressed as the product of the phase angles $\boldsymbol{\theta}$ and the power line-specific susceptance matrix $\boldsymbol{\Phi}$, is limited in both directions by the transmission capacities $\boldsymbol{\Omega}$ (Eq. 1c). Finally, the phase angle of one node is fixed to provide a reference for all other phase angles (Eq. 1d). Overall, the electricity generation $\boldsymbol{P}$ and the phase angles $\boldsymbol{\theta}$ at the different nodes are the only variables of the direct current load flow model.

2.2. Locational marginal emission factors

The mathematical derivation of locational MEFs is similar to the derivation of spatially-resolved marginal electricity prices used for nodal pricing and was first introduced with the conceptual work of Ruiz and Rudkevich [43]. We adapt the approach to our model formulation in vector form to provide the basis for the subsequent application of the ranging method.

The overall system emissions $\boldsymbol{E}$ result from the generator-specific emissions $\boldsymbol{e}^{\mathrm{T}}$ of the electricity generation $\boldsymbol{P}$. A constant efficiency of electricity generation is assumed to maintain the linear problem formulation. Thus, the correlation between overall system emissions and electricity generation is expressed as a linear equation:

$$\boldsymbol{E} = \boldsymbol{e}^{\mathrm{T}}\boldsymbol{P} \tag{2}$$

The change in overall system emissions due to the change in electricity demand is determined at the cost optimum of the optimization problem (marked in the following with *). Since the overall system emissions are a function of the electricity generation $\boldsymbol{E} = \boldsymbol{f}(\boldsymbol{P})$ and the energy balance (Eq. 1a) states that $\boldsymbol{P} = \boldsymbol{f}(\boldsymbol{D})$, the change of emissions $\mathrm{d}\boldsymbol{E}$ by the change in electricity demand $\mathrm{d}\boldsymbol{D}$ can be formulated based on Eq. 3. as follows:

$$\left(\frac{\mathrm{d}\boldsymbol{E}}{\mathrm{d}\boldsymbol{D}}\right)^{*} = \left(\frac{\mathrm{d}\boldsymbol{E}}{\mathrm{d}\boldsymbol{P}}\frac{\mathrm{d}\boldsymbol{P}}{\mathrm{d}\boldsymbol{D}}\right)^{*} = \boldsymbol{e}^{\mathrm{T}}\left(\frac{\mathrm{d}\boldsymbol{P}}{\mathrm{d}\boldsymbol{D}}\right)^{*} \tag{3}$$

In other words, the change in emissions $\mathrm{d}\boldsymbol{E}$ due to a change in demand $\mathrm{d}\boldsymbol{D}$ corresponds to the change in electricity generation $\mathrm{d}\boldsymbol{P}$ due to a change in demand $\mathrm{d}\boldsymbol{D}$ multiplied with the (constant) generator-specific emission factors. Since the specific emissions $\boldsymbol{e}^{\mathrm{T}}$ are known, the change of electricity generation $\mathrm{d}\boldsymbol{P}$ due to a change in electricity demand $\mathrm{d}\boldsymbol{D}$ needs to be determined. For this purpose, methods from optimization theory are applied [7]: Slack variables $\boldsymbol{s}$ are introduced into the optimization problem, such that all inequality constraints become equality constraints. The introduction of the slack variables results in a system of linear equations which contains more variables than constraints. As the optimization problem has more variables than constraints, optimization theory splits the variables $\boldsymbol{P}$, $\boldsymbol{\theta}$, and $\boldsymbol{s}$ into a set of basic variables (index B) with values greater than zero and a set of non-basic variables (index N) that are zero. The number of basic variables equals the number of constraints. Feasible solutions for the optimization problem can be found for different sets of basic variables. However, only one set of basic variables defines the cost-optimum. Based on an operational optimization, the set of optimal basic variables $(\boldsymbol{P}_{\mathrm{B}}\ \boldsymbol{\theta}_{\mathrm{B}}\ \boldsymbol{s}_{\mathrm{B}})^{\mathrm{T},*}$ and the corresponding non-basic variables $(\boldsymbol{P}_{\mathrm{N}}\ \ \boldsymbol{\theta}_{\mathrm{N}}\ \ \boldsymbol{s}_{\mathrm{N}})^{\mathrm{T},*}$ can be determined. These optimal basic and non-basic variables are the cost-optimal variables that satisfy the constraints of the optimization problem (Eqs. 1a-1d):

$$\boldsymbol{B}^{*}\begin{pmatrix}\boldsymbol{P}_{\mathrm{B}}\\ \boldsymbol{\theta}_{\mathrm{B}}\\ \boldsymbol{s}_{\mathrm{B}}\end{pmatrix}^{*} + \boldsymbol{N}^{*}\begin{pmatrix}\boldsymbol{P}_{\mathrm{N}}\\ \boldsymbol{\theta}_{\mathrm{N}}\\ \boldsymbol{s}_{\mathrm{N}}\end{pmatrix}^{*} = \begin{pmatrix}\boldsymbol{D}\\ \boldsymbol{\Gamma}\\ \boldsymbol{\Omega}\end{pmatrix}, \begin{pmatrix}\boldsymbol{P}_{\mathrm{B}}\\ \boldsymbol{\theta}_{\mathrm{B}}\\ \boldsymbol{s}_{\mathrm{B}}\end{pmatrix}^{*} \geq \boldsymbol{0}, \begin{pmatrix}\boldsymbol{P}_{\mathrm{N}}\\ \boldsymbol{\theta}_{\mathrm{N}}\\ \boldsymbol{s}_{\mathrm{N}}\end{pmatrix}^{*} = \boldsymbol{0} \tag{4}$$

The optimal basis matrix $\boldsymbol{B}^{*}$ and the optimal non-basis matrix $\boldsymbol{N}^{*}$ include the respective parameters of the constraints. The optimal basis matrix $\boldsymbol{B}^{*}$ is quadratic and non-singular, i.e., its determinant is non-zero, while the non-basis matrix $\boldsymbol{N}^{*}$ is generally non-quadratic. Since the non-basic variables are zero, they define which positivity constraints ($\boldsymbol{P}_{\mathrm{N}}, \boldsymbol{\theta}_{\mathrm{N}} = \boldsymbol{0}$) and which operational constraints ($\boldsymbol{s}_{\mathrm{N}} = \boldsymbol{0}$) of the optimization problem are binding, i.e., which constraints are active at the optimum. An infinitesimal change in demand does not change the set of binding or non-binding constraints [29], e.g., a power plant already operating at its capacity limit (= binding constraint) will still operate at its capacity limit while a power plant that is not operating at full capacity (= non-binding constraint) can change its electricity generation. As the sets of binding and non-binding constraints do not change, the sets of optimal basic and non-basic variables remain unchanged.

Therefore, in case of a change in demand, the non-basic variables are still zero ($\mathrm{d}\boldsymbol{P}_\mathbf{N}, \mathrm{d}\boldsymbol{\theta}_\mathbf{N}, \mathrm{d}\boldsymbol{s}_\mathbf{N} = \mathbf{0}$). Summarizing the relevant consequence of the applied optimization theory, only the basic variables respond to a change in demand and, thus, need to be considered for the derivative in Eq. 4.

The change of the optimal basic variables $(\,\mathrm{d}\boldsymbol{P}_\mathbf{B} \quad \mathrm{d}\boldsymbol{\theta}_\mathbf{B} \quad \mathrm{d}\boldsymbol{s}_\mathbf{B}\,)^{\mathrm{T},*}$ by an infinitesimal change of the demand $\mathrm{d}\boldsymbol{D}$ can be determined by differentiating Eq. 5. As only the electricity demand $\boldsymbol{D}$ is changed, the change in generation capacities $\mathrm{d}\boldsymbol{\Gamma}$ and transmission capacities $\mathrm{d}\boldsymbol{\Omega}$ can be set to zero (Eq. 6) and the derivative of the electricity generation according to the demand can be calculated (Eq. 7):

$$\begin{pmatrix} \mathrm{d}\boldsymbol{P}_\mathbf{B} \\ \mathrm{d}\boldsymbol{\theta}_\mathbf{B} \\ \mathrm{d}\boldsymbol{s}_\mathbf{B} \end{pmatrix}^{*} = \boldsymbol{B}^{*-1} \begin{pmatrix} \mathrm{d}\boldsymbol{D} \\ \mathrm{d}\boldsymbol{\Gamma} = \mathbf{0} \\ \mathrm{d}\boldsymbol{\Omega} = \mathbf{0} \end{pmatrix} \tag{5}$$

$$\left(\frac{\mathrm{d}\boldsymbol{P}_\mathbf{B}}{\mathrm{d}\boldsymbol{D}}\right)^{*} = \widetilde{\boldsymbol{B}^{*-1}} \tag{6}$$

The matrix $\widetilde{\boldsymbol{B}^{*-1}}$ consist of the first α columns (corresponding to the length of the vector $\boldsymbol{D}$) and of the first β rows (corresponding to the length of the vector $\boldsymbol{P}_\mathbf{B}$) of the matrix $\boldsymbol{B}^{*-1}$. Finally, the locational MEFs are obtained as the change of emissions due to a change in demand based on Eqs. 4 and 7:

$$\boldsymbol{MEF} = \left(\frac{\mathrm{d}\boldsymbol{E}}{\mathrm{d}\boldsymbol{D}}\right)^{*} = \left(\frac{\mathrm{d}\boldsymbol{E}}{\mathrm{d}\boldsymbol{P}_\mathbf{B}}\frac{\mathrm{d}\boldsymbol{P}_\mathbf{B}}{\mathrm{d}\boldsymbol{D}}\right)^{*} = \boldsymbol{e}_\mathbf{B}^{\mathrm{T}}\left(\frac{\mathrm{d}\boldsymbol{P}_\mathbf{B}}{\mathrm{d}\boldsymbol{D}}\right)^{*} = \boldsymbol{e}_\mathbf{B}^{\mathrm{T}}\widetilde{\boldsymbol{B}^{*-1}} \tag{7}$$

In Eq. 8, only the specific emissions of the basic variables $\boldsymbol{P}_\mathbf{B}$ are used as the non-basic variables $\boldsymbol{P}_\mathbf{N}$ are zero. The results of the MEFs are only valid as long as the sets of basic and non-basic variables remains unchanged, i.e., until an increase or reduction in demand would result in an optimal point that is bounded by a different set of constraints. We use this restriction in the MEF calculation to determine validity ranges for the locational MEFs in the next subsection.

2.3. Validity ranges

The validity ranges give a range for the maximum demand decrease $\Delta\boldsymbol{D}^{\mathbf{min}}$ and increase $\Delta\boldsymbol{D}^{\mathbf{max}}$ for which the locational MEFs remain constant.

$$\Delta\boldsymbol{D}^{\mathbf{min}} \leq \Delta\boldsymbol{D} \leq \Delta\boldsymbol{D}^{\mathbf{max}} \tag{8}$$

We determine the validity range of the locational MEFs by using the linear optimization method of ranging [7] that we briefly describe in the following.

As an infinitesimal change in demand does not change the set of binding and non-binding constraints, the locational MEFs remain constant as long as the set of binding constraints and, thus, the set of basic variables, does not change. In order to determine when the set of basic variables change, the derivative of the linear equation system (Eq. 6) can be slightly reformulated by first summarizing all optimal basic variables $(\,\boldsymbol{P}_\mathbf{B} \quad \boldsymbol{\theta}_\mathbf{B} \quad \boldsymbol{s}_\mathbf{B}\,)^{\mathrm{T},*}$ in the vector $\boldsymbol{x}_\mathbf{B}^{*}$. Then, the absolute change in the variables $\Delta\boldsymbol{x}_\mathbf{B}^{*}$ can be determined by an absolute change in the demand $\Delta\boldsymbol{D}$:

$$\Delta\boldsymbol{x}_B^{*} = \widehat{\boldsymbol{B}^{*-1}}\Delta D, \boldsymbol{x}_\mathbf{B}^{*} \geq \mathbf{0} \tag{9}$$

The matrix $\widehat{\boldsymbol{B}^{*-1}}$ contains the first α columns of $\boldsymbol{B}^{*-1}$ (length of the vector $\boldsymbol{D}$). The vector form of Eq. 10 can be transformed into parametric form to calculate the absolute change of any basic variable $\Delta x_{\mathrm{B},f}^{*}$ by the absolute change in demand at a specific node ΔD_g.

$$\Delta x_{B,f}^{*} = \widehat{B_{f,g}^{*-1}}\Delta D_g, \forall f \in F, \forall g \in G \tag{10}$$

The index $f \in F$ describes all basic variables while the index $g \in G$ defines the nodes. The parameters $\widehat{B_{f,g}^{*-1}}$ result from the optimal basic matrix $\boldsymbol{B}^{*}$ which includes the required parameters to satisfy the constraints summarized in Eq. 5. The set of basic variables holds true as long as the positivity constraint is fulfilled (see Eq. 5):

$$x_{\mathrm{B},f}^{*} + \Delta x_{\mathrm{B},f}^{*} > 0, \forall f \in F \tag{11}$$

Since Eq. 12 is an inequality and $\widehat{B_{f,g}^{*-1}}$ can have negative or positive values, a lower and an upper bound are obtained for ΔD_g when Eqs. 11 and 12 are combined. For negative values of $\widehat{B_{f,g}^{*-1}}$, Eqs. 11 and 12 provide an upper bound for ΔD_g and for positive values of $\widehat{B_{f,g}^{*-1}}$, they provide a lower bound. Thus, over all basic variables, a set of upper and lower bounds is obtained. In order to determine the overall boundaries for the change in demand ΔD_g, the maximum lower bound and minimum upper bound needs to be determined from the respective set of boundaries. The resulting boundaries provide the validity ranges of the locational MEFs for the linear dispatch model:

$$\sup_f\left(\frac{-x_{\mathrm{B},f}^{*}}{\widehat{B_{f,g}^{*-1}}} : \widehat{B_{f,g}^{*-1}} > 0\right) \leq \Delta D_g \leq \inf_f\left(\frac{-x_{\mathrm{B},f}^{*}}{\widehat{B_{f,g}^{*-1}}} : \widehat{B_{f,g}^{*-1}} < 0\right), \forall g \in G \tag{12}$$

The complete derivation of the bounds provided in Eq. 13 is shown in the Supplementary Information. As the methods for determining locational MEFs (Section 2.2) and their validity ranges (Section 2.3) are based on the optimal operation of the electric power system, the operation of the electric power system is not affected by the provided methods. Thus, the methods can be applied in optimization problems without changing the results.

3. Case study: German electric power system model

We apply the locational MEFs and the validity ranges on a model of the German electric power system due to its heterogeneous distribution of energy-intensive industries and renewable electricity generation. The model of the German electric power system is implemented in the SecMOD framework, a framework for energy system optimization that is formulated on the basis of the direct current load flow model [41]. The model of the German electric power system has a grid structure consisting of nodes where an electricity demand is defined and where power plants based on renewable and fossil energy carriers are modelled with their respective efficiencies. Each node of the model represents a different location in the German electric power system. Furthermore, connections are modelled that can be used to transmit electricity between the nodes. The spatial resolution results from the structure of the high voltage grid. Nodes represent locations where power plants, storage units, substations, and phase changers are connected to the grid and connections represent the actual 220 kV and 380 kV transmission cables. Overall, the model of the electric power system has a spatial resolution of 369 nodes, connected by power lines of the high voltage grid, and a temporal resolution of 8760 time steps per year. Furthermore, the electric power system is modelled as an island system, thus, neglecting electricity imports and exports across the border. For the analysis, we consider two scenarios: The current system based on historical data and a future system which is based on a capacity expansion optimization.

We parametrize the model of the current electric power system based on historical data of the year 2020 with node- and time-specific electricity generation capacities, efficiencies, and availabilities. The electricity demand is derived as time-specific, but spatially aggregated data from the ENTSO-E transparency platform [10]. We allocate the aggregated German electricity demand to the nodes according to the gross domestic product of the administrative districts in Germany as energy demand and economic growth show high correlation [22]. The detailed description of the allocation method is provided in the Supplementary Information.

Capacities and efficiencies of power plants and storage units are provided by the Marktstammdatenregister of the German Bundesnetzagentur [5] and Open Power System Data [54]. All availabilities, except for photovoltaics and wind power, are based on the assumptions of the ELMOD-DE model by Egerer et al. [8]. As the availabilities of photovoltaics are weather-dependent and no data is provided for temporally and spatially resolved availabilities in 2020, we determine the availabilities based on the electricity generation of the photovoltaic cells from the Photovoltaic Geographical Information System [11] and the respective photovoltaic capacities. The availabilities of wind power are calculated based on wind velocities from the Copernicus European Regional ReAnalysis model [46], converted to a hub height of 130 m and the power curve of an Enercon E115/3000 wind turbine. Further information on the model parametrization and calculation methods are provided in the Supplementary Information.

Fuel costs are provided by the International Energy Agency [23] and Egerer et al. [8]. The fuel-specific direct CO_2 emission factors are based on the Intergovernmental Panel on Climate Change [26]. The carbon price in the current system is 24.83 €/t, based on averaged data of 2020 [51]. Marginal operating costs of a power plant $i \in I$ are calculated with the following equation:

$$c_i^{op} = \frac{c_i^{fuel} + c^{CO_2} \bullet e_i}{\eta_i}, \forall i \in I \tag{13}$$

The marginal operating cost c_i^{op} are determined by the sum of the fuel price c_i^{fuel} and the carbon price c^{CO_2} multiplied with the generator-specific direct CO_2 emissions e_i divided by the power plants' efficiency η_i. Thus, the model provides generator-specific operating cost and emissions. The power plant capacities with operating cost and direct CO_2 emissions are represented in the merit order in Fig. 2.

For the future electric power system, we determine power plant capacities based on the model of the current German electric power system. We maintain all parameters from the current power system, except the carbon price and the electricity generation capacities. The carbon price is set to 129 €/t, based on assumptions for 2030 [37]. We determine the capacity expansion by optimizing investment and operating cost under consideration of capacity limits for the future electric power system. The investment cost are based on the model assumptions of Baumgärtner et al. [3]. The capacity limits of nuclear and coal power plants are set to zero as the nuclear phase out is already achieved and the German Government strives for a coal phase out until 2030 [15]. Furthermore, capacities of waste incineration, biogas power, hydropower, pumped hydro storage and power lines are set according to the existing capacities. The resulting future electric power system primarily has an additional generation capacity of 43.7 GW of wind turbines and 16.1 GW of natural gas power plants (specific capacity data and merit order are provided in the Supplementary Information).

4. Results and discussion

We analyze the locational MEFs in the current and the future electric power system on a representative winter and summer day. For the winter day, we chose the 9th of January and for the summer day the 9th of July. The winter day has a high availability of wind power, which is the renewable electricity generation technology with the highest locational differences in capacity, while the summer day has a low availability of wind power. Thus, the considered days represent one day with high and one day with low locational differences in electricity generation. For our analysis, we first compare the locational differences at noon on the winter and summer day (Section 4.1). In Section 4.2, we discuss the temporal development of the MEFs over the two days for one node in northern Germany and one node in southern Germany and provide the validity ranges of a demand decrease and increase. Then, we analyze the validity ranges of the locational MEFs at different locations in Germany in order to analyze the applicability of locational MEFs for the environmental assessment of load shifting (Section 4.3). Finally, we discuss the limitations of this work (Section 4.4).

4.1. Locational differences of marginal emission factors

We compare the locational MEFs at noon on the winter and summer day in the current and future electric power system of Germany (Fig. 3). Grid congestions are also shown as congestions are the cause for locational differences in the MEFs (when no grid congestion occurs, the locational MEFs are equal for every node). For the current electric power system, the MEFs show locational differences due to congestions, particularly on the winter day. On the winter day (Fig. 3a), the MEFs vary between a minimum of −84 g_{CO2}/kWh and a maximum of 998 g_{CO2}/kWh between different nodes. Thus, the emissions differ significantly with the location at which the change in demand occurs.

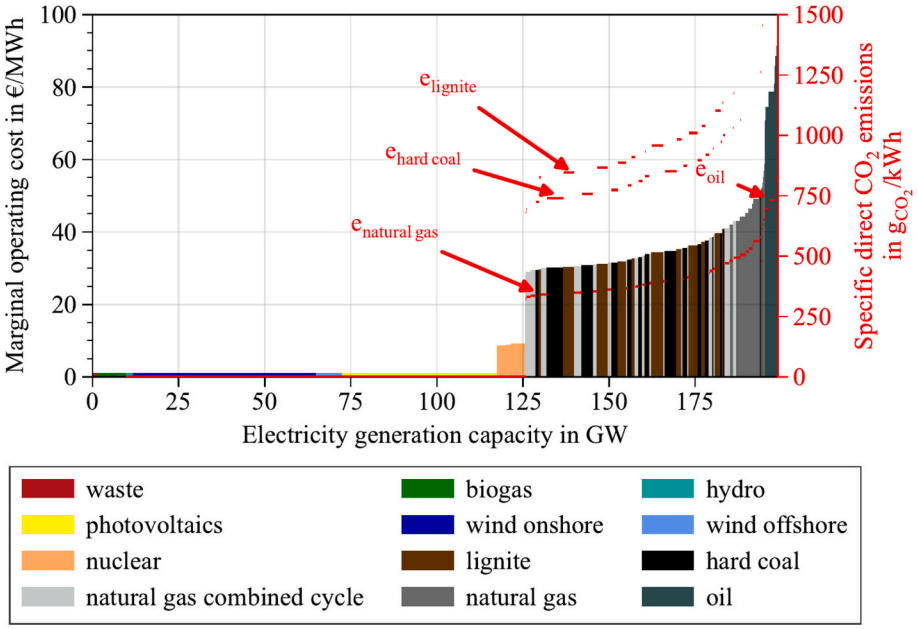

Fig. 2. Merit order of the current electric power system with marginal operating cost c_i^{op} and specific direct CO_2 emissions e_i of the power plants.

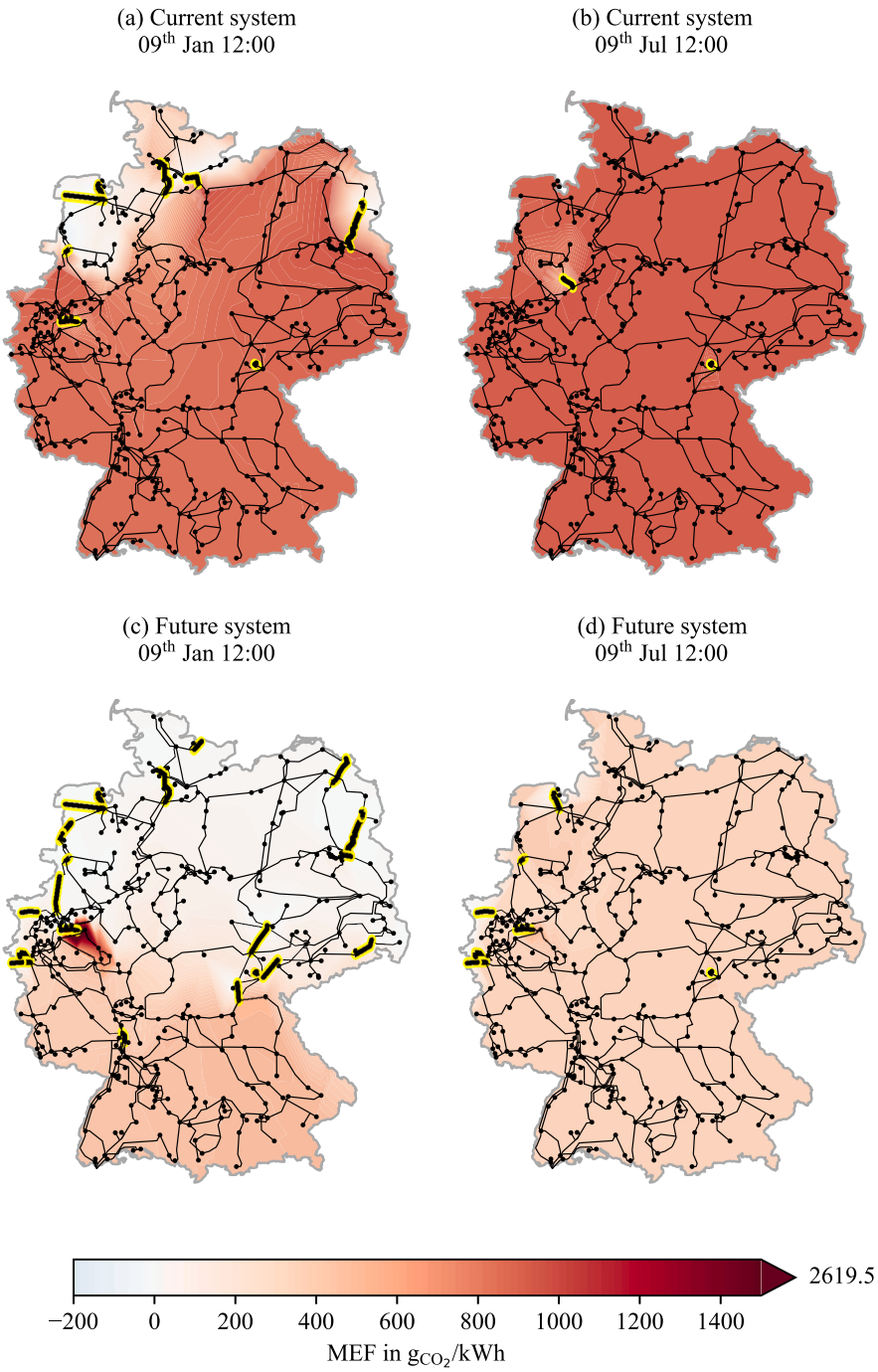

Fig. 3. Map of locational marginal emission factors (MEFs) in the German electric power system for the current electric power system on a winter day (a) and summer day (b), and for a future electric power system on a winter day (c) and summer day (d). The color indicates the locational MEFs: Light blue indicates a low emission factor, red indicates a high emission factor. Furthermore, grid congestion of power lines is shown by a bold line with a yellow border. (For interpretation of the references to color in this figure legend, the reader is referred to the web version of this article.)

Furthermore, the locational MEFs exceed the minimal and maximal specific emission factors of the power plants at some locations. The reason for the exceptionally low and high MEFs is the interconnectivity of the power grid: An increase in demand at a specific node can not only result in an increase in electricity generation by one power plant, but also require a decrease in electricity generation by other power plants in order to comply with the transmission limit constraints of the direct current load flow model (Eq. 1c). The same effect is also observed in nodal pricing [53]. However, nodal pricing generally results in lower price fluctuations across different locations compared to locational MEFs. The reason for the lower price fluctuations is the merit order: While grid congestions result in the operation of a power plant with slightly higher cost, the generator-specific emissions can be significantly higher or lower depending on which electricity generation technology is used. The strong fluctuations of locational MEFs due to grid congestion emphasize the importance to consider locational-aspects in the environmental assessment of load shifting.

On the summer day (Fig. 3b), the MEFs have a lower locational variation due to fewer grid congestions and range between a minimum of 535 g_{CO2}/kWh and a maximum of 936 g_{CO2}/kWh. The reason for the

comparably high emission factors is that overall electricity generation by renewables is very low on the considered summer day and additional electricity demand is covered by fossil-based power plants.

For the future electric power system (Fig. 3c and d), the MEFs vary between −144 g_{CO2}/kWh and 2620 g_{CO2}/kWh on the winter day and between 0 g_{CO2}/kWh and 561 g_{CO2}/kWh on the summer day. Compared to the current electric power system, the locational MEFs are generally lower in the future system as a higher amount of renewable energy sources provides electricity and no coal power plants are operated. However, locational differences of the MEFs increase as more congestions occur in the future system.

Thus, the differences in grid congestions between the current and future electric power systems show the correlation between grid congestions and the variations in locational MEFs: While the locational MEFs are equal when no grid congestion occurs, the variation of the locational MEFs increases with the extent of grid congestion. The greater number of congestions in the future electric power system results from the capacity expansion of wind turbines in northern Germany, which leads to an increased locational mismatch between electricity supply and demand.

4.2. Temporal differences and validity ranges of marginal emission factors

For a detailed comparison of the locational MEFs over the course of one day, we compare the MEFs at one node in northern Germany (Hamburg = H) and one node in southern Germany (Munich = M) for the winter day in the current and the future electric power system (Fig. 4). Furthermore, we provide the validity ranges of the locational MEFs in Fig. 4 to analyze the potential demand decrease and increase for which the MEFs remain constant.

In the current system (Fig. 4a), the MEF for Hamburg varies between 201 g_{CO2}/kWh and 965 g_{CO2}/kWh while the MEF for Munich varies between 232 g_{CO2}/kWh and 854 g_{CO2}/kWh. At the beginning of the day (0:00 a.m. until 4:00 a.m.), both MEFs are equal as no grid congestions occurs in the German electric power system and the marginal power plant is the same natural gas power plant for both nodes. However, the MEFs begin to differ from 5:00 a.m., with a maximum difference of 295 g_{CO2}/kWh between both nodes on the afternoon. The validity ranges ΔD_g of the locational MEFs differ for Hamburg and Munich at every hour and also show a high variation over the day: For Hamburg, the validity ranges are between 6.0 MW and 420.3 MW for a demand decrease and between 0.1 MW and 177.4 MW for a demand increase, while the ranges for Munich are between 3.2 MW and 188.7 MW for a demand decrease and between 0.1 MW and 95.0 MW for a demand increase. Generally, the validity ranges are limited by the ramping potential of power plants, i.e. ramping down until no electricity is generated or ramping up to the capacity limit, or by the potential transmission between two nodes, i.e. transmitting electricity until the capacity limit is reached. At the beginning of the day (0:00 a.m. until 4:00 a.m.), no grid congestion occurs and the validity ranges for Hamburg and Munich are the same as the validity ranges result from the ramping potential of the gas power plant that is the marginal power plant for both nodes. As for the MEFs, the validity ranges for both nodes start to differ from 5:00 a.m. If the MEFs between nodes are different, the validity ranges of the MEFs are typically also limited by different power plants or transmission lines, resulting in different validity ranges for the MEFs. While the validity ranges for both nodes can also be limited by the ramping or transmission potential of the same power plant or transmission line, respectively, the validity ranges still differ between the nodes due to the consequences of grid congestions on the overall electricity transmission.

In the future electric power system (Fig. 4b), the MEF for Hamburg varies between 42 g_{CO2}/kWh and 481 g_{CO2}/kWh while the MEF for Munich varies between 404 g_{CO2}/kWh and 799 g_{CO2}/kWh. Compared to the current electric power system, the MEF for Hamburg is significantly lower in the future system. The reason for the low MEF is the increased amount of electricity provided by wind power plants in northern Germany. In contrast, the MEF in Munich does not differ significantly

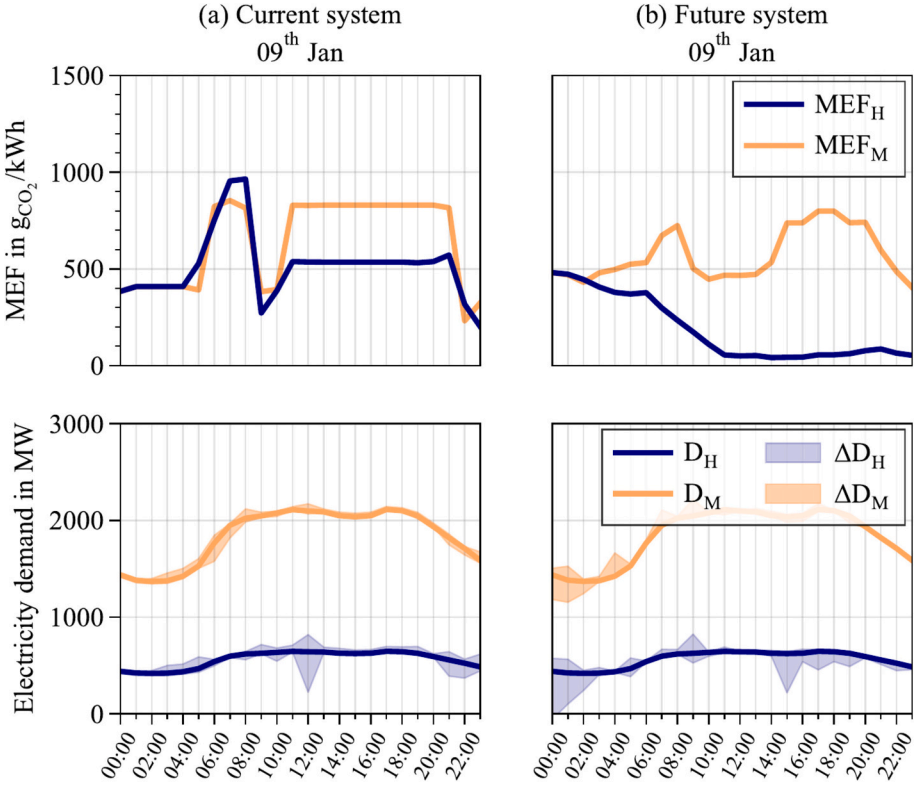

Fig. 4. Marginal emission factors (MEF) in Hamburg (H) and Munich (M) over the winter day for the current (a) and the future (b) electric power system. The ranges ΔD_g show the maximal decrease or increase in demand D_g at node g for which the MEFs remain constant.

between the current and the future electric power system as congestions in the electric power system inhibit the electricity transport to southern Germany. The validity ranges in Hamburg allow for a minimum demand decrease between 1.1 MW and 496.5 MW and a minimum increase in demand between 3.6 MW and 198.7 MW. In Munich, the ranges for a demand decrease are between 0.8 MW and 254.0 MW and for a demand increase between 0.4 MW and 240.0 MW. Thus, for Hamburg and Munich, the validity ranges in the future electric power system are similar to the validity ranges in the current system. Overall, the validity ranges differ significantly between every time step and are, furthermore, not necessarily limited by regionally close power plants or transmission lines, e.g., the validity ranges in Munich are limited by a power plant in North Germany at one time step and in the next time step the ranges are limited by a transmission line in South Germany. Therefore, the validity ranges do not show any systematic regional or temporal pattern over the course of one day and no conclusions can be derived for the environmental assessment of load shifting in different regions. However, if the demand is increased or decreased beyond the validity ranges at one of the nodes, the MEF at that node can change. Therefore, load shifting can only be assessed with the locational MEFs while the provided ranges are adhered to.

The MEFs of the summer day show lower variations and higher validity ranges for both the current and the future system (as shown in the Supplementary Information). The reason for the lower variations of the MEFs are fewer congestions occurring on the summer day. Fewer congestions also result in higher validity ranges as less transmission capacities limit the validity ranges. However, the validity ranges are not generally higher in the summer season as more congestion can occur on other summer days. Furthermore, due to the few congestions on the summer day in the current electric power system, the MEFs and the validity ranges for Hamburg and Munich are the same for most of the day. The MEFs only differ slightly between 11:00 a.m. and 1:00 p.m. due to grid congestions. These grid congestions also result in variations of the validity ranges.

Overall, the validity ranges are limited by different power plants and transmission lines at every location and time step and no key factors can be derived that systematically influence the validity ranges. However, high validity ranges at a specific time step generally result from a fossil-based marginal power plant that is reacting to a change in demand because the ranges correlate with the ramping potential of the power plants. The ramping potential is usually higher for fossil-based power plants as the plant capacity of fossil-based power plants is mostly higher compared to renewable power plants.

Comparing the environmental impact of load shifting at different locations is only possible if the amount of shifted load is inside the validity range at the considered locations. Therefore, in the next section, we assess the validity ranges of the MEFs for all locations in the electric power system.

4.3. Validity ranges in Germany

For assessing the applicability of the locational MEFs for the environmental assessment of load shifting at all locations in Germany, we determine the strictest validity ranges over the winter and summer day in the current and future electric power system. In Fig. 5, we provide the validity ranges at all locations in form of the minimal demand decrease and increase for which the MEFs are exact.

In the current system, the validity ranges for the demand increase are almost zero on the winter day (Fig. 5a) while the ranges for the demand decrease are mostly around 5 MW. On the summer day (Fig. 5b), the ranges are around 5 MW for the demand increase and 30 MW for the demand decrease. The reasons for the higher validity ranges on the summer day are fewer grid congestions and lower electricity generation by wind power plants, which results in large coal-based power plants setting the limiting constraints. Large coal-based power plants as the limiting constraints lead to high validity ranges since they can cover a greater demand margin. Furthermore, on the summer day, congestion influences the validity ranges in the north-west of Germany, resulting in low validity ranges in this region compared to the rest of Germany.

In the future electric power system, the validity ranges on the winter

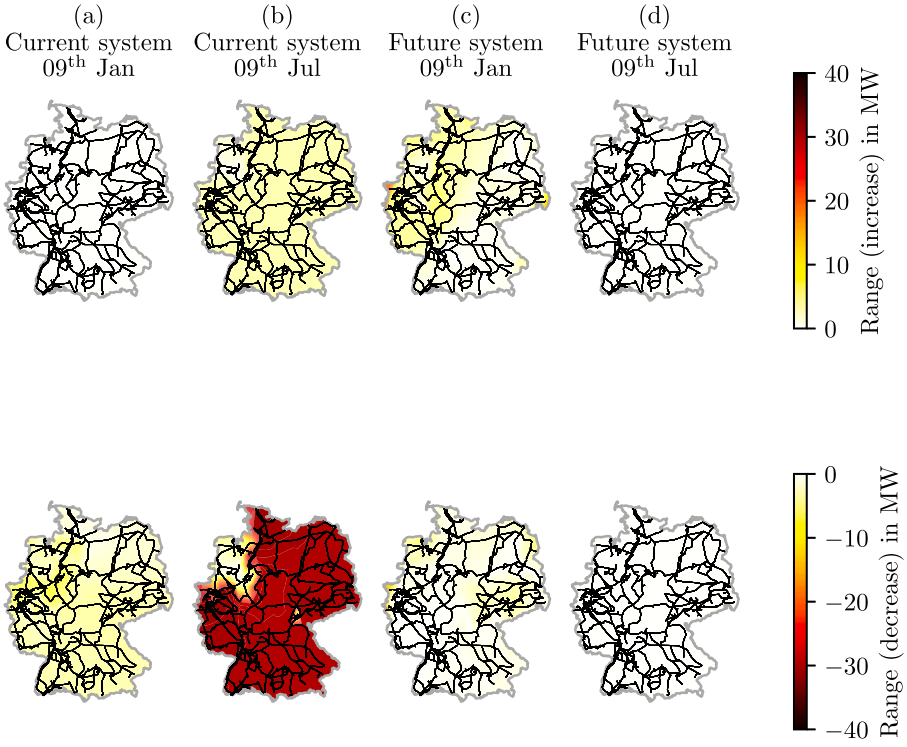

Fig. 5. Map of validity ranges for a demand decrease and increase in Germany for the current system on a winter day (a) and summer day (b), and for the future system on a winter day (c) and summer day (d). The color indicates the value of the locational validity ranges.

day (Fig. 5c) are mostly higher for the demand increase and lower for the demand decrease compared to the current system. However, for both the demand increase and decrease, the validity ranges are higher at the border regions of Germany. This is due to the congestions that occur in the border regions separating parts with high validity ranges from parts with lower ones. On the summer day (Fig. 5d), the validity ranges are nearly zero at all locations in Germany. The reason for the low validity ranges compared to the current system is the marginal electricity generation by natural gas power plants with small capacities that provide a strict limit.

The validity ranges in Germany are summarized in Table 1. Overall, the validity ranges for a demand decrease and increase are low at many locations compared to the load shifting capacity of current large-scale electric battery projects with around 20 MW of electric power [30]. Therefore, the locational MEFs are not generally applicable to assess the environmental impact of load shifting at any location in the system, but must be analyzed in combination with the validity ranges at the specific location. As best practice, we would advise to include the analysis of validity ranges into environmental assessment studies using locational MEFs and to validate if the assessed electric load shifting lies inside the validity ranges.

4.4. Limitations of this work

The design of the future electric power system is uncertain and depends on various future developments. As grid expansion is often slow, we have assumed for the future system that there will be no grid expansion, but also that electricity demand will remain constant. Furthermore, the expansion for the future electric power system mostly considers wind power as a renewable resource due to its low construction costs while photovoltaics are not expanded. However, the results of the MEFs and validity ranges in the future electric power system are representative for an electric power system with a high amount of low-carbon energy and more grid congestions compared to the current system, which are the relevant aspects of the future scenario.

Furthermore, the model does not consider ramping and start-up constraints of the power plants. Gas power plants have a fast response time in the range of minutes [21] and ramping and start-up is negligible in our hourly resolved model. The consideration of ramping and start-up for coal power plants would change the locational MEFs, as the part load behavior of the power plants results in different generator-specific emissions. Furthermore, the additional constraints would narrow the validity ranges. Additionally, the generator-specific emissions $\boldsymbol{e}^{\mathrm{T}}$ in Eq. 3 are constant in linear optimization problems, such as the direct current load flow model. However, part-load behavior of power plants results in non-constant generator-specific emissions, which can be included in the optimization problem by a piecewise-linearized formulation of the generator-specific emissions $\boldsymbol{e}^{\mathrm{T}}$ derived from a piecewise-linearized power plant efficiency. The piecewise-linearized formulation results in a mixed-integer linear problem that is not solvable in computational time. Furthermore the piecewise linearization results in smaller validity ranges as the piecewise linearization results in a multiplication of the linear constraint.

Apart from that, the direct current load flow model does not consider transmission losses. Transmission losses would result in smaller validity ranges as capacity limits of electricity generation and transmission would be reached faster, when the demand is changed. However, transmission losses in Germany are around 4 % [44] and, thus, would not have a significant impact on the results.

Despite the assumptions discussed, our work provides a robust method for quantifying the validity ranges of locational MEFs and highlights the limitations of their applicability for the environmental assessment of load shifting through demand-side management and electrical storage.

Table 1
Validity ranges for the current and future electric power system in Germany for the winter and summer day.

Validity range	Winter day	Summer day
Current system	Increase: 0.06–0.12 MW Decrease: 0.31–8.51 MW	Increase: 0.11–3.20 MW Decrease: 0.14–31.41 MW
Future system	Increase: 0.02–20.30 MW Decrease: 0–16.50 MW	Increase: 0.07–0.25 MW Decrease: 0.02–0.22 MW

5. Conclusion

For the location-specific environmental assessment of load shifting, locational marginal emission factors (MEFs) are utilized in literature. However, the locational MEFs are only valid for an infinitesimal change in demand. In this work, we provide validity ranges for MEFs in order to analyze their applicability for the environmental assessment of load shifting. The validity ranges are determined by using the method of ranging and applied to an optimal power flow model of the German electric power system.

Our results show that the locational MEFs vary between −144 g_{CO2}/kWh and 2620 g_{CO2}/kWh when congestion occurs. Thus, the locational MEFs even exceed power-plant-specific emission factors or reach negative values due to the interconnectivity of the power grid. Furthermore, the locational MEFs show significant differences between northern and southern Germany, particularly for the future power system in which the power grid is not expanded. Therefore, our work demonstrates the importance to consider locational MEFs in the environmental assessment of load shifting. The validity ranges for the locational MEFs are mostly around 5 MW, and even reach zero at some locations. Since large load shifts, as in current electric battery projects, can exceed the validity ranges, locational MEFs are not generally applicable for the environmental assessment of load shifting. Thus, the validity ranges must be taken into account when load shifting is assessed with locational MEFs. Besides, locational MEFs and their validity ranges are also relevant for a location-specific environmental assessment of other electricity consuming applications, such as heat pumps. However, in order to assess the environmental impacts of large load shifts and electricity consumers in a location-specific, valid and accessible way, further research is necessary.

CRediT authorship contribution statement

B. Nilges: Writing – original draft, Visualization, Methodology, Investigation, Data curation, Conceptualization. **A. Haese:** Writing – review & editing, Visualization, Software, Methodology, Investigation, Data curation. **C. Reinert:** Writing – review & editing, Supervision, Methodology, Conceptualization. **N. von der Assen:** Writing – review & editing, Supervision, Methodology, Funding acquisition, Conceptualization.

Declaration of competing interest

The authors declare that they have no known competing financial interests or personal relationships that could have appeared to influence the work reported in this paper.

Data availability

Data will be made available on request.

Appendix A. Supplementary data

Supplementary data to this article can be found online at https://doi.org/10.1016/j.apenergy.2024.125069.

References

[1] Alikhani P, Brinkel N, Schram W, Lampropoulos I, van Sark W. Marginal emission factors in power systems : The case of the Netherlands. In: proceedings of the 12th international conference on smart cities and green ICT systems; 2023. https://doi.org/10.5220/0011855700003491.

[2] Baumgärtner N, Delorme R, Hennen M, Bardow A. Design of low-carbon utility systems: exploiting time-dependent grid emissions for climate-friendly demand-side management. Appl Energy 2019;247:755–65. https://doi.org/10.1016/j.apenergy.2019.04.029.

[3] Baumgärtner N, Deutz S, Reinert C, Nolzen N, Kuepper LE, Hennen M, et al. Life-cycle assessment of sector-coupled National Energy Systems: environmental impacts of electricity, heat, and transportation in Germany till 2050. Front Energy Res 2021;9:886. https://doi.org/10.3389/fenrg.2021.621502.

[4] Böing F, Regett A. Hourly CO2 emission factors and marginal costs of Energy carriers in future multi-Energy systems. Energies 2019;12(12):2260. https://doi.org/10.3390/en12122260.

[5] Bundesnetzagentur. Marktstammdatenregister. 2024. Retrieved from, https://www.marktstammdatenregister.de.

[6] Chalendar JA, Benson SM. Why 100% renewable Energy is not enough. Joule 2019;3(6):1389–93. https://doi.org/10.1016/j.joule.2019.05.002.

[7] Cottle RW, Thapa MN. Linear and nonlinear optimization. In: Springer. 253. NY: New York; 2017.

[8] Egerer J, Gerbaulet C, Ihlenburg R, Kunz F, Reinhard B, von Hirschhausen C, et al. Electricity sector data for policy-relevant modeling: Data documentation and applications to the German and european electricity markets. 2014.

[9] Engstam L, Janke L, Sundberg C, Nordberg Å. Grid-supported electrolytic hydrogen production: cost and climate impact using dynamic emission factors. Energy Convers Manag 2023;293:117458. https://doi.org/10.1016/j.enconman.2023.117458.

[10] ENTSO-E. Transparancy Platform. 2024. Retrieved from, https://transparency.entsoe.eu/.

[11] European Commission. Photovoltaic Geographical Information System (PVGIS). 2016. Retrieved from, https://re.jrc.ec.europa.eu/pvg_tools/de/.

[12] Fleschutz M, Bohlayer M, Braun M, Henze G, Murphy MD. The effect of price-based demand response on carbon emissions in European electricity markets: the importance of adequate carbon prices. Appl Energy 2021;295:117040. https://doi.org/10.1016/j.apenergy.2021.117040.

[13] Fleschutz M, Bohlayer M, Braun M, Murphy MD. From prosumer to flexumer: case study on the value of flexibility in decarbonizing the multi-energy system of a manufacturing company. Appl Energy 2023;347:121430. https://doi.org/10.1016/j.apenergy.2023.121430.

[14] Garcia R, Freire F. Marginal life-cycle greenhouse gas emissions of electricity generation in Portugal and implications for electric vehicles. Resources 2016;5(4):41. https://doi.org/10.3390/resources5040041.

[15] German Government. Mehr Fortschritt wagen – Bündnis für Freiheit. Gerechtigkeit und Nachhaltigkeit; 2021.

[16] Germscheid, S. H.M., Nilges, B., Assen, N. Von Der, Mitsos, A., Dahmen, M. (2024). Optimal design of a local renewable electricity supply system for power-intensive production processes with demand response. Comput Chem Eng, 185, 108656. doi: https://doi.org/10.1016/j.compchemeng.2024.108656.

[17] Graff Zivin JS, Kotchen M, Mansur ET. Spatial and temporal heterogeneity of marginal emissions: Implications for electric cars and other electricity-shifting policies. 2014. p. 2014. https://doi.org/10.1016/j.jebo.2014.03.010.

[18] Hawkes AD. Estimating marginal CO2 emissions rates for national electricity systems. Energy Policy 2010;38(10):5977–87. https://doi.org/10.1016/j.enpol.2010.05.053.

[19] He H, Rudkevich A, Li X, Tabors R, Derenchuk A, Centolella P, et al. Using marginal emission rates to optimize investment in carbon dioxide displacement technologies. Electr J 2021;34(9):107028. https://doi.org/10.1016/j.tej.2021.107028.

[20] Heffron R, Körner M-F, Wagner J, Weibelzahl M, Fridgen G. Industrial demand-side flexibility: a key element of a just energy transition and industrial development. Appl Energy 2020;269:115026. https://doi.org/10.1016/j.apenergy.2020.115026.

[21] Hentschel J, Babić U, Spliethoff H. A parametric approach for the valuation of power plant flexibility options. Energy Rep 2016;2:40–7. https://doi.org/10.1016/j.egyr.2016.03.002.

[22] Huang B-N, Hwang MJ, Yang CW. Causal relationship between energy consumption and GDP growth revisited: a dynamic panel data approach. Ecol Econ 2008;67(1):41–54. https://doi.org/10.1016/j.ecolecon.2007.11.006.

[23] IEA. World energy outlook 2021. Paris. 2021. https://doi.org/10.1787/14fcb638-en.

[24] IEA. World energy outlook 2021. Paris. 2022. https://doi.org/10.1787/3a469970-en.

[25] ILCD. ILCD handbook - general guide on LCA - detailed guidance. 2010.

[26] IPCC. Guidelines for national greenhouse gas inventories: Volume 2: Energy - chapter 2: Stationary combustion. 2006.

[27] Kelley MT, Baldick R, Baldea M. Demand response operation of electricity-intensive chemical processes for reduced greenhouse gas emissions: application to an air separation unit. ACS Sustain Chem Eng 2019;7(2):1909–22. https://doi.org/10.1021/acssuschemeng.8b03927.

[28] Kopsakangas-Savolainen M, Mattinen MK, Manninen K, Nissinen A. Hourly-based greenhouse gas emissions of electricity – cases demonstrating possibilities for households and companies to decrease their emissions. J Clean Prod 2017;153:384–96. https://doi.org/10.1016/j.jclepro.2015.11.027.

[29] Kuhn HW, Tucker AW, editors. Linear inequalities and related systems. Princeton University Press: Princeton; 1956.

[30] Energy Kyon. Batteriespeicherprojekte von Kyon energy. 2024. Retrieved from, https://www.kyon-energy.de/referenzen.

[31] Li Y, Yang X, Du E, Liu Y, Zhang S, Yang C, et al. A review on carbon emission accounting approaches for the electricity power industry. Appl Energy 2024;359:122681. https://doi.org/10.1016/j.apenergy.2024.122681.

[32] Lindberg J, Lesieutre BC, Roald LA. Using geographic load shifting to reduce carbon emissions. Electr Power Syst Res 2022. https://doi.org/10.1016/j.epsr.2022.108586.

[33] Lund H, Mathiesen BV, Christensen P, Schmidt JH. Energy system analysis of marginal electricity supply in consequential LCA. Int J Life Cycle Assess 2010;15(3):260–71. https://doi.org/10.1007/s11367-010-0164-7.

[34] Lund PD, Lindgren J, Mikkola J, Salpakari J. Review of energy system flexibility measures to enable high levels of variable renewable electricity. Renew Sust Energ Rev 2015;45:785–807. https://doi.org/10.1016/j.rser.2015.01.057.

[35] Oates DL, Spees K. Locational marginal emissions: A force multiplier for the carbon impact of clean energy programs. 2022.

[36] Park B, Dong J, Liu B, Kuruganti T. Decarbonizing the grid: utilizing demand-side flexibility for carbon emission reduction through locational marginal emissions in distribution networks. Appl Energy 2023;330:120303. https://doi.org/10.1016/j.apenergy.2022.120303.

[37] Pietzcker RC, Osorio S, Rodrigues R. Tightening EU ETS targets in line with the European green deal: impacts on the decarbonization of the EU power sector. Appl Energy 2021;293:116914. https://doi.org/10.1016/j.apenergy.2021.116914.

[38] Pimm AJ, Palczewski J, Barbour ER, Cockerill TT. Using electricity storage to reduce greenhouse gas emissions. Appl Energy 2021;282:116199. https://doi.org/10.1016/j.apenergy.2020.116199.

[39] Purchala K, Meeus L, van Dommelen D, Belmans R. Usefulness of DC power flow for active power flow analysis. In: IEEE power engineering society general meeting; 2005. p. 2457–62. https://doi.org/10.1109/PES.2005.1489581.

[40] Regett A, Boing F, Conrad J, Fattler S, Kranner C. Emission assessment of electricity: mix vs. marginal power plant method. In: 15th international conference on the European Energy market (EEM); 2018. p. 1–5. https://doi.org/10.1109/EEM.2018.8469940.

[41] Reinert C, Schellhas L, Mannhardt J, Shu DY, Kämper A, Baumgärtner N, et al. SecMOD: an open-source modular framework combining multi-sector system optimization and life-cycle assessment. Front Energy Res 2022;10:884525. https://doi.org/10.3389/fenrg.2022.884525.

[42] Rudkevich A, Ruiz PA, Carroll RC. Locational carbon footprint and renewable portfolio policies: a theory and its implications for the eastern interconnection of the US. In: 44th Hawaii international conference on system sciences; 2011. p. 1–12. https://doi.org/10.1109/HICSS.2011.287.

[43] Ruiz PA, Rudkevich A. Analysis of marginal carbon intensities in constrained power networks. In: Proceedings of the 43rd Hawaii international conference on system sciences; 2010. p. 1–9. https://doi.org/10.1109/HICSS.2010.59.

[44] Sadovskaia K, Bogdanov D, Honkapuro S, Breyer C. Power transmission and distribution losses – a model based on available empirical data and future trends for all countries globally. Int J Electr Power Energy Syst 2019;107:98–109. https://doi.org/10.1016/j.ijepes.2018.11.012.

[45] Santecchia A, Castro-Amoedo R, Nguyen T-V, Kantor I, Stadler P, Maréchal F. The critical role of electricity storage for a clean and renewable European economy. Energy Environ Sci 2023. https://doi.org/10.1039/D3EE02768F.

[46] Schimanke S, Ridal M, Le Moigne P, Berggren L, Undén P, Randriamampianina R, et al. CERRA sub-daily regional reanalysis data for Europe on single levels from 1984 to present. 2021.

[47] Seckinger N, Radgen P. Dynamic prospective average and marginal GHG emission factors—scenario-based method for the German power system until 2050. Energies 2021;14(9):2527. https://doi.org/10.3390/en14092527.

[48] Siler-Evans K, Azevedo IL, Morgan MG. Marginal emissions factors for the U.S. electricity system. Environ Sci Technol 2012;46(9):4742–8. https://doi.org/10.1021/es300145v.

[49] Summerbell DL, Khripko D, Barlow C, Hesselbach J. Cost and carbon reductions from industrial demand-side management: study of potential savings at a cement plant. Appl Energy 2017;197:100–13. https://doi.org/10.1016/j.apenergy.2017.03.083.

[50] Thind MPS, Wilson EJ, Azevedo IL, Marshall JD. Marginal emissions factors for electricity generation in the midcontinent ISO. Environ Sci Technol 2017;51(24):14445–52. https://doi.org/10.1021/acs.est.7b03047.

[51] Umweltbundesamt (2023). Preisentwicklung für Emissionsberechtigungen (EUA) seit 2008.

[52] Valenzuela LF, Degleris A, El Gamal A, Pavone M, Rajagopal R. Dynamic locational marginal emissions via implicit differentiation. IEEE Trans Power Syst 2023:1138–47. https://doi.org/10.1109/TPWRS.2023.3247345.

[53] Weber C, Möst D, Fichtner W. Economics of power systems. Cham, Switzerland: Springer International Publishing; 2022.

[54] Weibezahn J, Weinhold R, Gerbaulet C, Kunz F. List of conventional power plants in Germany and European countries. 2024. Retrieved from, https://data.open-power-system-data.org/conventional_power_plants/2020-10-01.

[55] Wolf I, Holzapfel PKR, Meschede H, Finkbeiner M. On the potential of temporally resolved GHG emission factors for load shifting: a case study on electrified steam generation. Appl Energy 2023;348:121433. https://doi.org/10.1016/j.apenergy.2023.121433.